Analysis of steady-state performance for cross-directional control

A.G. Wills and W.P. Heath

Abstract: The authors analyse the steady-state behaviour of a class of cross-directional controllers that are pertinent to general web-forming processes. Their analysis is framed in terms of the controllable space prescribed by the interaction matrix and general discrete orthonormal basis descriptions of both the input and output space under the assumption of closed-loop stability. The specific choice of controller defines (whether explicitly or implicitly) an additional assumed controlled space. It is well known that the controllable space determines a lower bound on output variation. They examine the implications of integral action and provide sufficient conditions for the steady-state output variation to achieve this lower bound. They confirm some intuitive results that connect the optimal constrained and unconstrained steady-state solutions for model-based control with no model mismatch. Model mismatch is usually detrimental to steady-state performance. This effect is interpreted in terms of leakage between the controllable and assumed controlled spaces, as well as their respective orthogonal complements.

1 Introduction

A web-forming process is the term usually associated with the class of industrial processes where the primary objective is to produce a thin sheet of material in a continuous strip. Some examples of such processes are paper-making machines, steel rolling mills and plastic film extrusion systems. Associated with most web-forming processes are a number of quality constraints that must be met to satisfy customer demands. Process disturbances require the use of feedback control strategies to maintain a desired level of quality. Online determination of quality satisfaction is usually achieved by measuring certain properties of the material. In some cases, e.g. paper making, these properties are coupled. The direction associated with the main flow of material or machine processing, is usually called the machine direction (MD), and the direction orthogonal to this is usually called the cross-direction (CD) [1, 2]. In this paper we are concerned with the regulation of a single CD property and assume that measurements have been sufficiently decoupled to allow independent analysis.

We are concerned with the steady-state behaviour of a class of controllers that are pertinent to regulating a single property of the CD. Several authors have proposed control strategies that utilise orthogonal basis functions [3–6]. The idea is to represent the output and/or input as a linear combination of the respective basis functions. This can provide an elegant method for selecting the significant modal content of the input and output, which has implications in terms of computational efficiency (see [4] and the references therein).

Fundamental limitations on the performance of any controller are provided in [3, 4]. It is shown that the steady-state actuator profile shape is crucial in determining a lower bound for output variation. The basic idea is to partition the output space into controllable and uncontrollable subspaces. The lower bound is reached if we can set the controllable part of the output to zero. In the current work, we consider the case of a model-based controller design with no model mismatch and confirm some intuitive results that link the constrained and unconstrained problems. Various practical aspects such as model mismatch, limited control authority and the requirement to ensure robustness, prevent us from achieving the lower bound for output variation. We consider in detail the steady-state behaviour of a model-based controller with model mismatch, under the assumption of closed-loop stability.

2 Preliminaries

2.1 Notation and definitions

This section establishes some preliminary notation and definitions that are helpful in describing the CD control problem for general web-forming processes. For a broad outline of web-forming processes see [1, 2]. It should be stated from the outset that we will make a number of simplifying assumptions in order to describe CD behaviour. However, the assumptions we make have received wide acceptance in the CD control community [3, 7–10]. Therefore, we consider the following ideal model as the

IEE Proceedings online no. 20020471

DOI: 10.1049/ip-cta:20020471

Paper first received 4th June 2001 and in revised form 6th April 2002

A.G. Wills is with School of Electrical Engineering and Computer Science, University of Newcastle, Callaghan, NSW 2308, Australia
E-mail: ony@eecsmail.newcastle.edu.au

W.P. Heath is with Centre for Integrated Dynamics And Control (CIDAC), University of Newcastle, Callaghan, NSW 2308, Australia

'best' approximation to the true plant with respect to the selected model structure. Furthermore, we consider an estimated model as the result of some identification process, and assume that both the estimated and ideal models are a good representation of the true plant behaviour, at least in steady state. The following ideal model of CD behaviour is meant as a reference for analysis purposes and to reflect the generally accepted paradigm of ideal and estimated models of a system [11].

We consider discrete-time linear time-invariant models of CD behaviour. We assume that the MD and CD components have been decoupled, and make no further reference to the coupling that exists between MD and CD in reality [10]. Similarly, we are considering CD variation in only one profile property. Therefore, we will not treat the case of regulating multiple, and usually coupled, profile properties (e.g. coupling between calliper profile and moisture profile [12]). Furthermore, we assume that the output is represented as a vector of equally spaced measurements across the strip and is available in discrete time intervals denoted as t. More formally, let $\mathbf{y}(t) \in \mathbb{R}^n$ denote the vector of discrete CD measurements at time t. Similarly, let $\mathbf{u}(t) \in \mathbb{R}^m$ denote the vector of actuator inputs at time t. Typically $n \times m$. Then the CD behaviour may be described as follows [3, 7–10],

$$\mathbf{y}(t) = G(z^{-1})\mathbf{B}\mathbf{u}(t) + \mathbf{d}(t) \tag{1}$$

Here $G(z^{-1})$ is a scalar transfer function that describes the dynamics (assumed to be the same for all actuators) and $\mathbf{d}(t) \in \mathbb{R}^n$ describes the disturbance across the strip at time t. Note that $G(z^{-1})$ will usually include a delay term. We assume that

$$\lim_{z^{-1} \to 1} G(z^{-1}) = G_{ss} \neq 0 \tag{2}$$

and G_{ss} is finite, i.e. a stable open-loop system. Since we are primarily concerned with the steady-state behaviour of (1) we will consider in detail the case where

$$\mathbf{d}(t) = \mathbf{d}_{ss} \tag{3}$$

where $\mathbf{d_{ss}} \in \mathbb{R}^n$ is constant and finite. The remaining term, $\mathbf{B} \in \mathbb{R}^{nm}$, is called the interaction matrix and describes the steady-state response of the actuators on the profile. It has been shown that the actuator response shape is crucial in determining the controllable and uncontrollable parts of the output [3, 4]. To describe this more formally, we start by defining some relevant spaces. Let the output space Y be defined as the Euclidean $\mathbb{R}^m$ space and the input space, U, be defined as the Euclidean $\mathbb{R}^m$ space. Then the controllable and uncontrollable subspaces are described as [4]

$$Y_c := \{\mathbf{y} \in Y : \exists \mathbf{u} \in U \text{ with } \mathbf{y} = \mathbf{B}\mathbf{u}\} \tag{4}$$

$$Y_{uc} := Y_c^{\perp} \tag{5}$$

Here the symbol, $\perp$, denotes the orthogonal complement such that

$$Y_c^{\perp} = \{\mathbf{y} \in Y : \mathbf{B}^T\mathbf{y} = 0\} \tag{6}$$

The above provides a fundamental limitation in terms of a lower bound for steady-state output variation as measured by $\|\mathbf{y}_{ss}\|_2$, which is a natural measure of performance. If at any time the output vector $\mathbf{y}(t)$ belongs to the uncontrollable space, Y_{uc}, then there is no other combination of inputs that will result in 'better' output performance. Note that any $\mathbf{y} \in Y$ can be represented as a linear combination of orthogonal vectors from Y_c and Y_{uc}, i.e. for

$$\mathbf{y} = \mathbf{y}^c + \mathbf{y}^{uc}, \ \exists \mathbf{u} \in U \text{ s.t.}$$
$$\mathbf{y}^c = \mathbf{B}\mathbf{u} \text{ and } \mathbf{B}^T\mathbf{y}^{uc} = 0 \tag{7}$$

Moreover, we have the following nominal bound for performance:

$$\|\mathbf{y}_{ss}\|_2 \geq \|\mathbf{y}_{ss}^{uc}\|_2 \tag{8}$$

In [3, 4] the controllable and uncontrollable subspaces are explicitly stated in terms of basis functions. The use of basis functions to describe the output space has been considered by several authors [3, 4, 6]. In some cases, basis functions have also been used to describe the input space [5]. Moreover, some basis function descriptions (e.g. spectral basis functions) provide an efficient representation of the output space Y, which has benefits in terms of reducing the computational load. In this paper, we are concerned with the general steady-state behaviour of a class of CD controllers that encompass all discrete orthonormal basis functions for the input and output spaces.

Remark 2.1.1: For clarity of exposition, we restrict our analysis to discrete orthonormal basis function descriptions. However, our analysis should be extendible to the more general case of orthogonal and/or continuous basis functions in a natural manner. More detail on continuous basis function descriptions is given in [3, 4].

We begin our discussion of the controller class by defining the discrete orthonormal basis functions for the input and output spaces. Let $\bar{\mathbf{V}} \in \mathbb{R}^{mm}$ be a unitary matrix, so that the column entries of $\bar{\mathbf{V}}$ form an orthonormal basis for the input space U. Likewise, let $\bar{\mathbf{W}} \in \mathbb{R}^{nn}$ be a unitary matrix, so that the column entries of $\bar{\mathbf{W}}$ form an orthonormal basis for the output space Y.

Next we define a convenient matrix partition that is used in the controller class definition, and throughout this paper in general. Let $\mathbf{A} \in \mathbb{R}^{qp}$ be a general matrix, then for $r \leq \min(q, p)$ we may partition $\mathbf{A}$ as

$$\mathbf{A} = \begin{bmatrix} \mathbf{A}_{11} & \mathbf{A}_{12} \\ \mathbf{A}_{21} & \mathbf{A}_{22} \end{bmatrix} \tag{9}$$

where $\mathbf{A}_{11} \in \mathbb{R}^{rr}$, $\mathbf{A}_{12} \in \mathbb{R}^{r(p-r)}$, $\mathbf{A}_{21} \in \mathbb{R}^{(q-r)r}$ and $\mathbf{A}_{22} \in \mathbb{R}^{(q-r)(p-r)}$.

For the unconstrained case, we define a class of linear controllers as follows.

Definition 2.1.1: Let $\mathbf{K}_r(z^{-1})$ be a class of controllers that satisfy the following, for $r \leq \bar{r}$

$$\mathbf{K}_r(z^{-1}) = -\bar{\mathbf{V}}\left[\frac{1}{1-z^{-1}}\mathbf{K}_I + \mathbf{K}_R(z^{-1})\right]\mathbf{T}\bar{\mathbf{W}}^T \tag{10}$$

where the mm matrix $\mathbf{K}_I$ is given by

$$\mathbf{K}_I = \begin{bmatrix} \bar{\mathbf{K}}_I & \mathbf{0} \\ \mathbf{0} & \mathbf{0} \end{bmatrix} \tag{11}$$

and the mm transfer function matrix $\mathbf{K}_R(z^{-1})$ is given by

$$\mathbf{K}_R(z^{-1}) = \begin{bmatrix} \bar{\mathbf{K}}_R(z^{-1}) & \mathbf{0} \\ \mathbf{0} & \mathbf{0} \end{bmatrix} \tag{12}$$

Here, $\tilde{\mathbf{V}}$ and $\tilde{\mathbf{W}}$ are unitary matrices as defined above and $\mathbf{T} \in \mathbb{R}^{mn}$ with rank $\bar{r}$. Furthermore, $\bar{\mathbf{K}}_I \in \mathbb{R}^{rr}$ is a diagonal matrix with nonzero diagonal elements and $\bar{\mathbf{K}}_R(z^{-1})$ is an rr rational transfer function matrix.

Remark 2.1.2: In this paper, we have assumed stability of the closed-loop system. It is well known that CD control systems may become unstable if the controller is poorly tuned. In particular, it has been observed that as r increases it may become harder to design a robust controller [8].

However, this paper is concerned with steady-state performance. Therefore, we consider the assumption of closed-loop stability as a necessary condition for the validity of the ensuing analysis. The analysis of stability is beyond the scope of this paper.

Consider the case where the columns of $\tilde{\mathbf{W}}$ form a spectral basis for Y and they are ordered (in some sense) by their 'smoothness'. Suppose we would like to represent the output with a limited combination of these basis vectors (thus performing a filter operation), a natural selection for $\mathbf{T}$ is a diagonal matrix with entries strictly greater than zero for diagonal elements up to and including the number of desired nodes. Where convenient, we may refer to $\mathbf{T}$ as the filter matrix. This idea is not foreign to the CD control community and has been suggested by several authors [3, 4, 8]. Another selection might be to let $\mathbf{T}$ be the pseudoinverse of $\mathbf{B}$ (if it exists), which projects the output onto the input space using a least-squares mapping. More generally if the singular value decomposition of $\mathbf{B}$ is $\mathbf{B}=\mathbf{WSV}^T$, we might let $\mathbf{T}=\mathbf{VS}^*\mathbf{W}^T$, where $\mathbf{S}^*$ is also diagonal, and such that the diagonal elements of $\mathbf{S}^*\mathbf{S}$ are either 1 or 0. Occasionally, it will be convenient to express $\mathbf{T}^T$ using a QR factorisation. This is usually written as

$$\mathbf{T}^T = \mathbf{QR} \tag{13}$$

where $\mathbf{Q}\in\mathbb{R}^{nn}$ is a unitary matrix and $\mathbf{R}\in\mathbb{R}^{nm}$ is an upper triangular matrix [13].

3 Steady-state behaviour

3.1 Effect of integral action

This Section introduces a convenient expression for the steady-state behaviour of the class of CD controllers given in (10) as applied to the general web-forming process described by (1). A block diagram of the closed-loop system can be found in Fig. 1. It should be noted that this is a regulator problem. The accompanying interpretation of this expression reflects the generally acknowledged result that spectral basis functions are well suited for CD control problems [3, 4, 8]. A further observation provides sufficient conditions for the steady-state output to achieve the lower bound on our measure of performance.

With reference to Fig. 1, it is straightforward to write the closed-loop formula

$$\mathbf{y}(t) = [\mathbf{I} + G(z^{-1})\mathbf{B}\mathbf{K}_r(z^{-1})]^{-1}\mathbf{d}(t) \tag{14}$$

Then we have the following observation.

Observation 3.1.1: Let $\mathbf{Q}$ and $\mathbf{R}$ be given by the QR factorisation of $\mathbf{T}^T$ as defined in (13). For a controller, $\mathbf{K}_r(z^{-1})$, that satisfies (10) and ensures closed-loop stability of (14), then $\lim_{t\to\infty}\mathbf{y}(t)=\mathbf{y}_{ss}$ is given by

$$\mathbf{y}_{ss} = \tilde{\mathbf{W}}\begin{bmatrix}\mathbf{0} & \mathbf{0}\\ \mathbf{F} & \mathbf{I}_{n-r}\end{bmatrix}\tilde{\mathbf{W}}^T\mathbf{d}_{ss} \tag{15}$$

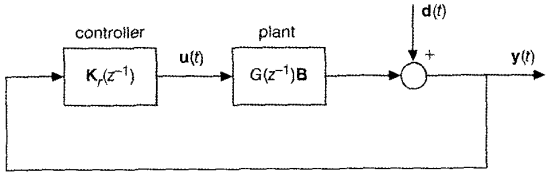

Fig. 1 *Block diagram of CD control system*

where

$$\bar{\mathbf{W}} = \tilde{\mathbf{W}}\mathbf{Q} \tag{16}$$

and $\mathbf{I}_{n-r}$ is the $(n-r)(n-r)$ identity matrix. Furthermore,

$$\mathbf{F} = -\bar{\mathbf{B}}_{21}\bar{\mathbf{B}}_{11}^{-1} \tag{17}$$

where the indices indicate submatrices as obtained by applying (9), and

$$\bar{\mathbf{B}} = \tilde{\mathbf{W}}^T\mathbf{B}\tilde{\mathbf{V}} \tag{18}$$

Proof: Since $\mathbf{T}^T=\mathbf{QR}$ and $\tilde{\mathbf{W}}$ is unitary, we may write (14) as

$$\mathbf{y}(t) = \tilde{\mathbf{W}}\left\{\mathbf{I} + G(z^{-1})\bar{\mathbf{B}}\left[\frac{1}{1-z^{-1}}\mathbf{K}_I + \mathbf{K}_R(z^{-1})\right]\mathbf{R}^T\right\}^{-1}\tilde{\mathbf{W}}^T\mathbf{d}(t) \tag{19}$$

Using the matrix partition defined in (9) we have

$$\mathbf{y}(t) = \tilde{\mathbf{W}}\begin{bmatrix}\mathbf{C}_{11}(z^{-1}) & \mathbf{0}\\ \mathbf{C}_{21}(z^{-1}) & \mathbf{I}\end{bmatrix}^{-1}\tilde{\mathbf{W}}^T\mathbf{d}(t) \tag{20}$$

where

$$\mathbf{C}_{11}(z^{-1}) = \mathbf{I} + \frac{G(z^{-1})}{1-z^{-1}}\bar{\mathbf{B}}_{11}\bar{\mathbf{K}}_I\mathbf{R}_{11}^T + G(z^{-1})\bar{\mathbf{B}}_{11}\bar{\mathbf{K}}_R(z^{-1})\mathbf{R}_{11}^T \tag{21}$$

$$\mathbf{C}_{21}(z^{-1}) = -\frac{G(z^{-1})}{1-z^{-1}}\bar{\mathbf{B}}_{21}\bar{\mathbf{K}}_I\mathbf{R}_{11}^T - G(z^{-1})\bar{\mathbf{B}}_{21}\bar{\mathbf{K}}_R(z^{-1})\mathbf{R}_{11}^T \tag{22}$$

From (20)–(22) we obtain an expression for steady-state behaviour by taking the limit as $z^{-1}\to 1$, i.e.

$$\mathbf{y}_{ss} = \lim_{z^{-1}\to 1}\tilde{\mathbf{W}}\begin{bmatrix}[\mathbf{C}_{11}(z^{-1})]^{-1} & \mathbf{0}\\ \mathbf{C}_{21}(z^{-1})[\mathbf{C}_{11}(z^{-1})]^{-1} & \mathbf{I}\end{bmatrix}\tilde{\mathbf{W}}^T\mathbf{d}_{ss} \tag{23}$$

Since

$$\lim_{z^{-1}\to 1}[\mathbf{C}_{11}(z^{-1})]^{-1} = \mathbf{0} \tag{24}$$

$$\lim_{z^{-1}\to 1}\mathbf{C}_{21}(z^{-1})[\mathbf{C}_{11}(z^{-1})]^{-1} = -\bar{\mathbf{B}}_{21}\bar{\mathbf{B}}_{11}^{-1} \tag{25}$$

Hence the result □

The above observation provides a general expression for the steady-state behaviour of the closed-loop system described by (14). One interpretation of the above result is as follows. Consider $\tilde{\mathbf{W}}$ as an ortnonormal basis for Y. Then $\mathbf{W}^L\mathbf{y}_{ss}$ rotates $\mathbf{y}_{ss}$ into the basis coefficient space. From (15) we see that the first r 'modes' of $\mathbf{y}_{ss}$ are effectively cancelled, while the remaining $n-r$ 'modes' are affected by $\mathbf{F}$. We use the word 'modes' here with caution since $\bar{\mathbf{W}}=\tilde{\mathbf{W}}\mathbf{Q}$, and therefore, in general $\bar{\mathbf{W}}$ may not necessarily be a sensible basis for Y. We again stress that the above observation is based on the assumption of closed-loop stability, and therefore an arbitrary selection of $\bar{\mathbf{W}}$ may result in an unstable closed-loop system.

In the light of the above observation, consider the case where $\bar{\mathbf{W}}$ is a sensible basis for Y. For example, consider the case where the columns of $\bar{\mathbf{W}}$ form a spectral basis for Y and are ordered in terms of 'smoothness'. Then, in this case, cancelling the first r modes of $\mathbf{y}_{ss}$ is a natural objective.

Next we give sufficient conditions for the steady-state output to achieve the lower bound for our performance

measure. If the first m columns of $\bar{\mathbf{W}}$ form a basis for Y_c then we have the following observation.

Observation 3.1.2: Suppose span $\{\bar{\mathbf{w}}_1, \ldots, \bar{\mathbf{w}}_m\} = Y_c$, where $\bar{\mathbf{w}}_i$ denotes the ith column of $\bar{\mathbf{W}}$. Then for a controller, $\mathbf{K}_r(z^{-1})$, that satisfies (10) and ensures closed-loop stability of (14) with $r = m$, we have

$$\mathbf{y}_{ss} \in Y_{uc} \tag{26}$$

Proof: If span $\{\bar{\mathbf{w}}_1, \ldots, \bar{\mathbf{w}}_m\} = Y_c$ then by definition

$$\bar{\mathbf{W}}^T \mathbf{B} \tilde{\mathbf{V}} = \begin{bmatrix} \bar{\mathbf{B}}_{11} & \bar{\mathbf{B}}_{12} \\ \mathbf{0} & \mathbf{0} \end{bmatrix} \tag{27}$$

since

$$\langle \bar{\mathbf{w}}_i, \mathbf{Bu} \rangle = 0, \ \forall \mathbf{u} \in U \text{ and for } i = m+1, \ldots, n \tag{28}$$

In which case, $\bar{\mathbf{B}}_{21} = \mathbf{0}$ and therefore $\mathbf{F} = \mathbf{0}$. Then we have

$$\mathbf{y}_{ss} = \bar{\mathbf{W}} \begin{bmatrix} \mathbf{0} & \mathbf{0} \\ \mathbf{0} & \mathbf{I}_{n-m} \end{bmatrix} \bar{\mathbf{W}}^T \mathbf{d}_{ss} \tag{29}$$

To prove that $\mathbf{y}_{ss} \in Y_{uc}$ it is suffices to show that $\mathbf{B}^T \mathbf{y}_{ss} = \mathbf{0}$

$$\mathbf{B}^T \mathbf{y}_{ss} = \begin{bmatrix} \bar{\mathbf{B}}_{11}^T & \mathbf{0} \\ \bar{\mathbf{B}}_{12}^T & \mathbf{0} \end{bmatrix} \begin{bmatrix} \mathbf{0} & \mathbf{0} \\ \mathbf{0} & \mathbf{I}_{n-m} \end{bmatrix} \bar{\mathbf{W}}^T \mathbf{d}_{ss} \tag{30}$$

$$= \begin{bmatrix} \mathbf{0} & \mathbf{0} \\ \mathbf{0} & \mathbf{0} \end{bmatrix} \bar{\mathbf{W}}^T \mathbf{d}_{ss} \tag{31}$$

□

Remark 3.1.1: Since (26) is true, then (29) is the least squares solution to the steady-state control problem, i.e. $\mathbf{y}_{ss}$ is the projection of $\mathbf{d}_{ss}$ onto Y_{uc}.

Bearing in mind the controller structure defined by (10), this observation verifies that the first m columns of $\tilde{\mathbf{W}}$ are important in terms of steady-state performance.

3.2 Steady-state behaviour using singular value decomposition of ideal model

We now discuss the steady-state performance of controllers based on the singular value decomposition (SVD) of $\mathbf{B}$ [4, 8, 10]. We show for completeness, the intuitively obvious and generally accepted result that as we increase r, the output variation does not increase. Furthermore, in the limit when $r = m$ we achieve the lower bound for our measure of performance (as might be expected from Section 3.1). Moreover, we provide an example with a different choice of basis that also exhibits this behaviour. Following on from this, we discuss the case where actuators are bounded by hard constraints and show a similar result of monotonicity as r increases. We finish this Section with an example that illustrates these results.

To aid our discussion, we introduce some notation for the SVD of $\mathbf{B}$. The interaction matrix, $\mathbf{B}$, may be expressed as

$$\mathbf{B} = \mathbf{WSV}^T \tag{32}$$

where $\mathbf{W} \in \mathbb{R}^{nn}$ and $\mathbf{V} \in \mathbb{R}^{mm}$ are unitary matrices and the upper mm block of $\mathbf{S} \in \mathbb{R}^{nm}$ is a matrix containing the singular-values of $\mathbf{B}$ in nonincreasing order along the diagonal and all the remaining elements are zero. The SVD provides an elegant framework for selecting significant modes of $\mathbf{B}$. Let $\mathbf{B}_r$ denote the reduced modal version of $\mathbf{B}$ defined as follows:

$$\mathbf{B}_r = \mathbf{WS}_r \mathbf{V}^T \tag{33}$$

where $\mathbf{S}_r \in \mathbb{R}^{nm}$ is a matrix whose first r diagonal elements are the corresponding singular values of $\mathbf{B}$, placed in nonincreasing order and all other elements are zero. Using this notation, we may define the controlled space and its orthogonal complement, respectively, as

$$Y_c^r := \{\mathbf{y} \in Y : \exists \mathbf{u} \in U \ \text{ with } \ \mathbf{y} = \mathbf{B}_r \mathbf{u}\} \tag{34}$$

and

$$Y_{uc}^r := (Y_c^r)^{\perp} \tag{35}$$

where convenient, we may refer to Y_{uc}^r as the uncontrolled space.

We take this opportunity to stress the important difference between controlled and controllable modes of Y. The controllable modes are defined in Section 2.1 and describe a fundamental limitation on output variation, in terms of a lower bound. On the other hand, controlled modes are defined by the selection of basis vectors that are used in the formulation of a control design. In this particular case, we note that the controlled space is a subspace of the controllable space. For more general basis functions and/or model mismatch, this may not necessarily be true (see Section 3.3).

In Section 2.1 we have suggested a common and natural choice for $\mathbf{T}$ when using spectral basis functions to represent Y. To clarify our intentions, we restrict our analysis to the case where the left mm block of the filter matrix $\mathbf{T}$ is diagonal and all remaining elements of $\mathbf{T}$ are zero. More formally, let $\mathbf{T}$ be defined as

$$\mathbf{T} = \begin{bmatrix} \bar{\mathbf{T}} & \mathbf{0} \end{bmatrix} \in R^{mn} \tag{36}$$

where $\bar{\mathbf{T}} \in \mathbb{R}^{mm}$ is a diagonal matrix with the first r diagonal elements being strictly greater than zero. Furthermore, let $\tilde{\mathbf{W}} = \mathbf{W}$ and $\tilde{\mathbf{V}} = \mathbf{V}$, where $\mathbf{W}$ and $\mathbf{V}$ are defined in (32). This construction is analogous to selecting the first r columns (basis vectors) of $\tilde{\mathbf{W}}$ to represent the output. Comparing this case with observation 3.1.1 we find that $\mathbf{Q} = \mathbf{I}$, $\bar{\mathbf{W}} = \mathbf{W}$ and $\bar{\mathbf{B}} = \mathbf{S}$. Then we have the following observation.

Observation 3.2.1: For a controller, $\mathbf{K}_r(z^{-1})$, that satisfies (10), and ensures closed-loop stability of (14) with $\tilde{\mathbf{W}} = \mathbf{W}$, $\tilde{\mathbf{V}} = \mathbf{V}$ and $\mathbf{T}$ as defined in (36), then $\mathbf{y}_{ss}$ is given by

$$\mathbf{y}_{ss} = \mathbf{W} \begin{bmatrix} \mathbf{0} & \mathbf{0} \\ \mathbf{0} & \mathbf{I}_{n-r} \end{bmatrix} \mathbf{W}^T \mathbf{d}_{ss} \tag{37}$$

$$\mathbf{y}_{ss} \in Y_{uc}^r \tag{38}$$

where $\mathbf{I}_{n-r}$ is the $(n-r)$ $(n-r)$ identity matrix. Furthermore, we have

$$\|\mathbf{y}_{ss}^r\|_2 \geq \|\mathbf{y}_{ss}^{r+1}\|_2 \text{ for } r = 1, \ldots, m-1 \tag{39}$$

where $\mathbf{y}_{ss}^r$ denotes the steady-state output resulting from a controller with rank r.

Proof: Since $\mathbf{Q} = \mathbf{I}$, $\bar{\mathbf{W}} = \mathbf{W}$ and $\bar{\mathbf{B}} = \mathbf{S}$, we may write (14) as

$$\mathbf{y}(t) = \mathbf{W} \left\{ \mathbf{I} + \mathbf{S} \left[\frac{1}{1 - z^{-1}} \mathbf{K}_I + \mathbf{K}_R(z^{-1}) \right] \mathbf{T} \right\}^{-1} \mathbf{W}^T \mathbf{d}(t) \tag{40}$$

and following a similar argument to that for observation 3.1.1, we find that

$$\mathbf{y}_{ss} = \mathbf{W} \begin{bmatrix} \mathbf{0} & \mathbf{0} \\ \mathbf{0} & \mathbf{I}_{n-r} \end{bmatrix} \mathbf{W}^T \mathbf{d}_{ss} \tag{41}$$

To prove that $\mathbf{y}_{ss} \in Y_{uc}^r$ it is sufficient to show that $\mathbf{B}_r^T \mathbf{y}_{ss} = 0$. Since $\mathbf{B}_r^T = \mathbf{V}\mathbf{S}_r^T\mathbf{W}^T$ we have

$$\mathbf{V}\mathbf{S}_r^T\mathbf{W}^T\mathbf{y}_{ss} = \mathbf{V}\begin{bmatrix}\mathbf{S}_{11} & \mathbf{0}\\ \mathbf{0} & \mathbf{0}\end{bmatrix}\begin{bmatrix}\mathbf{0} & \mathbf{0}\\ \mathbf{0} & \mathbf{I}_{n-r}\end{bmatrix}\mathbf{W}^T\mathbf{d}_{ss} \quad (42)$$

$$= \mathbf{V}\begin{bmatrix}\mathbf{0} & \mathbf{0}\\ \mathbf{0} & \mathbf{0}\end{bmatrix}\mathbf{W}^T\mathbf{d}_{ss} \quad (43)$$

We can show that

$$\|\mathbf{y}_{ss}^r\|_2 \geq \|\mathbf{y}_{ss}^{r+1}\|_s \text{ for } r = 1, \ldots, m-1 \quad (44)$$

by observing from (37) that

$$\|\mathbf{y}_{ss}^r\|_2^2 = \sum_{i=r+1}^{n} \gamma_i^2 \quad (45)$$

where γ_i is the ith element of $\mathbf{W}^T\mathbf{d}_{ss}$, and therefore, increasing r reduces the number of terms in the summation. □

Remark 3.2.1: If we choose $r = m$ in the above, then the variation of $\mathbf{y}_{ss}$ achieves the lower bound for steady-state performance, i.e. $\mathbf{y}_{ss} \in Y_{uc}$. Note that for any $r < m$ we may incur a performance degradation. However, as shown in Section 3.3, in the case of model mismatch, increasing r does not necessarily provide better performance.

The above result is not unique to the SVD of $\mathbf{B}$. For the sake of brevity, we offer without proof, another choice of basis that exhibits this behaviour. Consider the case where $\mathbf{B}$ is represented by the QR factorisation, i.e.

$$\mathbf{B} = \mathbf{QR} \quad (46)$$

and let $\tilde{\mathbf{W}} = \mathbf{Q}$. Furthermore, let $\mathbf{T} = \mathbf{R}^T$, then comparing this case with observation 3.1.1, we find that $\tilde{\mathbf{W}} = \mathbf{Q}$ and $\tilde{\mathbf{B}} = \mathbf{R}\tilde{\mathbf{V}}$. Using a similar argument to that found in observation 3.2.1, we observe that the output variation is monotonically nonincreasing as r is increased.

3.2.1 Steady-state behaviour with hard constraints: A similar result can be obtained for the case where actuators are bounded by hard constraints. We assume without loss of generality that $G_{ss} = 1$. Furthermore, we suppose that the limited control authority can be represented as a set of linear inequality constraints on $\mathbf{u}_{ss}$. Then the reduced order optimal input vector can be found as follows. Let the cost function be defined as:

$$J(\mathbf{u}_{ss}) = \|\mathbf{y}_{ss}\|_2^2 \quad (47)$$

Then, we define the reduced mode cost function as

$$J_r(\mathbf{u}_{ss}) = \|\mathbf{B}_r\mathbf{u}_{ss} + \mathbf{d}_{ss}\|_2^2 \quad (48)$$

with $\mathbf{B}_r$ given by (33). Then the reduced order optimal solution can be found as follows. For some $r \leq m$ we have:

$$\mathbf{u}_{ss_r}^* = \arg\min_{\mathbf{u}_{ss} \in U_r} J_r(\mathbf{u}_{ss}) \text{ subject to } \mathbf{A}\mathbf{u}_{ss} \leq \mathbf{b} \quad (49)$$

where $U_r := \text{span}\{\mathbf{v}_1, \ldots, \mathbf{v}_r\}$ and $\mathbf{v}_i$ denotes the ith column vector of $\mathbf{V}$.

Remark 3.2.2: If the model $\mathbf{B}$ is known, a model predictive control strategy will reach $\mathbf{u}_{ss}^*$. Such controllers have been proposed by many authors for the CD problem [4, 14]. In particular, [4] gives an example of generalised predictive control (GPC) [15] where the output space is restricted with Chebyshev polynomials. There are a number of ways to implement integral action in model predictive control (MPC). In [16] a method is proposed where integral action is implemented via an observer for the disturbance, and two quadratic programs are solved at each control step. In particular, the steady-state cost is explicitly incorporated into the control strategy.

Note that since $\mathbf{u}_{ss_r}^* \in U_r$ we have

$$J(\mathbf{u}_{ss_r}^*) = J_r(\mathbf{u}_{ss_r}^*) \quad (50)$$

Therefore, we have the following observation.

Observation 3.2.2: For $J(\mathbf{u}_{ss})$ as defined in (47) and $\mathbf{u}_{ss}^*$, as defined in (49) then we have

$$J(\mathbf{u}_{ss_{r+1}}^*) \leq J(\mathbf{u}_{ss_r}^*) \quad (51)$$

Proof: This follows immediately since $\mathbf{u}_{ss_r}^* \in U_{r+1}$ □

Remark 3.2.3: Suppose we do not restrict $\mathbf{u}_{ss} \in U_r$ when minimising $J_r(\mathbf{u}_{ss})$. Then, in general, there exists a solution, say $\tilde{\mathbf{u}}_{ss} \notin U_r$, such that $J(\tilde{\mathbf{u}}_{ss}) < J(\mathbf{u}_{ss_r}^*)$. Such solutions are excluded for the sake of robustness [7]. In implementing a controller designed to satisfy (49), care must be taken to ensure that $\mathbf{u}_{ss}$ indeed lies in U_r.

If we wish to assess the performance of the constrained case, then we have the following observation.

Observation 3.2.3: Let $\tilde{\mathbf{u}}_{ss_r}^*$ denote the unconstrained solution to (49). Furthermore, let r^* be given by,

$$r^* = \arg\max r \text{ s.t. } J(\tilde{\mathbf{u}}_{ss_r}^*) = J(\mathbf{u}_{ss_r}^*). \quad (52)$$

Then we have the following lower and upper bounds for $J(\mathbf{u}_{ss_r}^*)$,

$$J(\tilde{\mathbf{u}}_{ss_r}^*) \leq J(\mathbf{u}_{ss_r}^*) \text{ for } r = 1, \ldots, m \quad (53)$$

$$J(\mathbf{u}_{ss_r}^*) \leq J(\mathbf{u}_{ss_{r^*}}^*) \text{ for } r = r^*, \ldots, m \quad (54)$$

Proof: The first bound (53) is self-evident and the second bound (54) comes from observation 3.2.2. □

We illustrate the above results with an example.

Example 1: In this example we are considering the model of a paper-machine with 101 actuators and 501 output measurements, both with and without actuator constraints. The steady-state actuator response shape is shown in Fig. 2*a*. Note that the shape is chosen to have zero area, and hence does not taper to zero at the edges. This is highly artificial, but ensures that any controller has no effect on MD variation. In practice care must be taken to limit MD/CD interaction. In the case of actuator constraints, we impose an absolute limit on actuator position as follows: $|u_i| \leq 1$ for $i = 1, \ldots, m$. We choose a controller, $\mathbf{K}_r(z^{-1})$, that satisfies (10), with $\tilde{\mathbf{W}} = \mathbf{W}$, $\tilde{\mathbf{V}} = \mathbf{V}$, where $\mathbf{W}$ and $\mathbf{V}$ are given by (32), and with $\mathbf{T}$ given by

$$\mathbf{T} = \begin{bmatrix}\mathbf{I} & \mathbf{0}\end{bmatrix} \in R^{mn} \quad (55)$$

Fig. 2*b* shows the output variation as a function of r for both cases. Note that for $r = 101$ we achieve the upper bound for output performance (i.e. the lower bound for output variation). Furthermore, we note that for $r \leq 15$, the output variation is the same for both cases, above this value, the unconstrained case performs better than the constrained case. In practice it is highly unlikely that such a bound is achievable, as the required input variation would be infeasible. This is illustrated by Fig. 2*c* which shows the corresponding input variation, it should be noted that it is shown on a logarithmic scale.

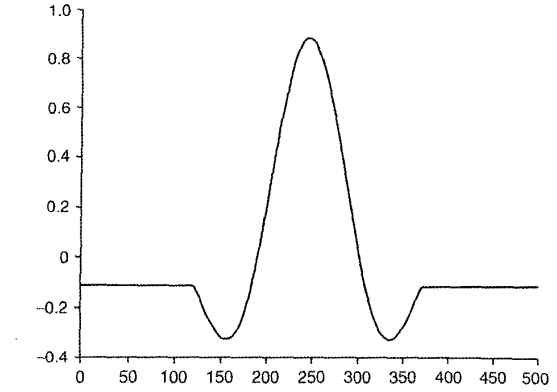

a

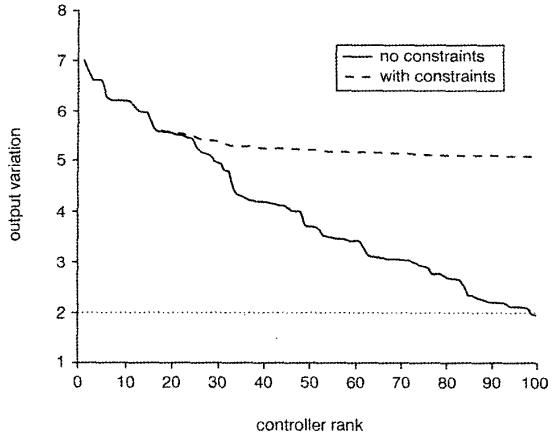

b

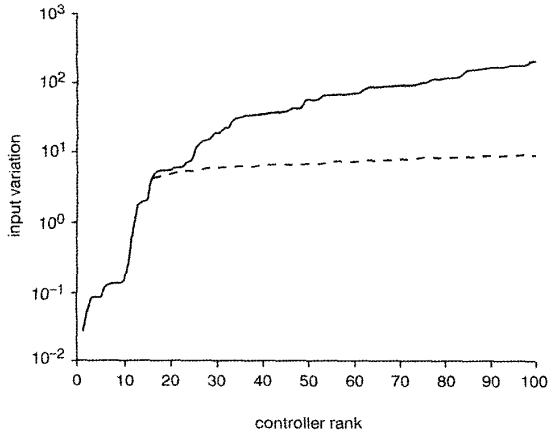

c

Fig. 2 *Steady-state variation with ideal model*

a actuator response shape from actuator no. 50. The shape is constructed using a truncated sine function

b output variation $\|\mathbf{y}_{ss}\|_2$ as a function of r. Dotted line across the Figure indicates the upper bound for performance for $r = 101$

c input variation $\|\mathbf{u}_{ss}\|_2$ as a function of r, on a logarithmic key as in *b*

3.3 Steady-state behaviour with model mismatch

This Section analyses the implications of model mismatch for steady-state performance of the closed-loop system described by (14). Model mismatch has been considered by several authors using various frameworks [8, 12]. The general idea is to design a controller that ensures robust stability for a norm-bounded additive term, say Δ, which represents the difference between the ideal and estimated models. Some other possibilities for modelling uncertainty are considered in [8].

We now attempt to offer some insight into the effects of model mismatch on steady-state performance, assuming closed-loop stability. We have found that the steady-state performance is affected by a leakage term that rotates controlled modes of the disturbance into uncontrolled modes of the output.

Since we are primarily concerned with the effects of model mismatch, we start by providing some relevant notation. Let $\hat{\mathbf{B}}$ denote the estimated interaction matrix and $\hat{G}(z^{-1})$ the estimated transfer function. Then in a similar way to (4) and (5), the estimated controllable and uncontrollable subspaces may be defined, respectively, as

$$\hat{Y}_c := \{\mathbf{y} \in Y : \exists \mathbf{u} \in U \text{ with } \mathbf{y} = \hat{\mathbf{B}}\mathbf{u}\} \tag{56}$$

and

$$\hat{Y}_{uc} := \hat{Y}_c^{\perp} \tag{57}$$

It is worth noting that in general, $\hat{Y}_c$ is not necessarily equal to Y_c. The implications of this will be discussed later in this Section.

Using the SVD, we may express $\hat{\mathbf{B}}$ as

$$\hat{\mathbf{B}} = \hat{\mathbf{W}}\hat{\mathbf{S}}\hat{\mathbf{V}}^T \tag{58}$$

Let $\mathbf{M}$ denote the isomorphism between $\mathbf{W}$ and $\hat{\mathbf{W}}$ defined as

$$\mathbf{M} = \mathbf{W}^T\hat{\mathbf{W}} \tag{59}$$

where $\mathbf{W}$ is defined in (32). Similarly, let $\mathbf{N}$ denote the isomorphism between $\mathbf{V}$ and $\hat{\mathbf{V}}$ defined as

$$\mathbf{N} = \mathbf{V}^T\hat{\mathbf{V}} \tag{60}$$

where $\mathbf{V}$ is also defined in (32). Then we may express $\mathbf{B}$ as

$$\mathbf{B} = \hat{\mathbf{W}}\mathbf{H}\hat{\mathbf{V}}^T \tag{61}$$

where

$$\mathbf{H} = \mathbf{M}^T\mathbf{S}\mathbf{N} \tag{62}$$

It will also be convenient to express $\hat{\mathbf{B}}$ as

$$\hat{\mathbf{B}} = \mathbf{B} + \Delta \tag{63}$$

where Δ represents the difference between the ideal and estimated models. Furthermore, let $\hat{\mathbf{B}}_r$, $\hat{Y}_c^r$ and $\hat{\mathbf{Y}}_{uc}^r$ be defined in the same manner as $\mathbf{B}_r$, Y_c^r and Y_{uc}^r (see (33)–(35), respectively).It is easily seen that the SVD description of $\mathbf{B}$ encompasses the more general orthonormal basis description through an appropriate isomorphism. We may express $\mathbf{B}$ as

$$\mathbf{B} = \tilde{\mathbf{W}}\tilde{\mathbf{B}}\tilde{\mathbf{V}}^T \tag{64}$$

where $\tilde{\mathbf{B}} = (\tilde{\mathbf{W}}^T\mathbf{B}\tilde{\mathbf{V}})$. Let us define the SVD of $\tilde{\mathbf{B}}$ as $\mathbf{W}_B\mathbf{S}\mathbf{V}_B^T$ (note that multiplication by a unitary matrix does not change the singular values), then

$$\mathbf{B} = \mathbf{W}\mathbf{S}\mathbf{V}^T \tag{65}$$

where $\mathbf{W} = (\tilde{\mathbf{W}}\mathbf{W}_B)$ and $\mathbf{V}^T = (\mathbf{V}_B^T\tilde{\mathbf{V}}^T)$, which is in the form of (32). This implies that the following analysis includes the case of more general basis functions, where the results may be interpreted through an appropriate isomorphism.

Then, for a controller based on the SVD of $\hat{\mathbf{B}}$ we have the following observation.

Observation 3.3.1: For a controller, $\mathbf{K}_r(z^{-1})$, that satisfies (10) and ensures closed-loop stability of (14) with $\tilde{\mathbf{W}} = \hat{\mathbf{W}}$, $\tilde{\mathbf{V}} = \hat{\mathbf{V}}$ and $\mathbf{T}$ as defined in (36), then $\mathbf{y}_{ss}$ is given by

$$\mathbf{y}_{ss} = \hat{\mathbf{W}} \begin{bmatrix} \mathbf{0} & \mathbf{0} \\ \mathbf{F} & \mathbf{I}_{n-r} \end{bmatrix} \bar{\mathbf{W}}^T \mathbf{d}_{ss} \tag{66}$$

$$\mathbf{y}_{ss} = \in \hat{Y}_{uc}^r \tag{67}$$

Here, $\mathbf{I}_{n-r}$ is the $(n-r)$ $(n-r)$ identity matrix and

$$\mathbf{F} = -\mathbf{H}_{21}\mathbf{H}_{11}^{-1} \tag{68}$$

where $\mathbf{H}$ is defined in (62). Furthermore, $\hat{\mathbf{W}}$ and $\hat{\mathbf{V}}$ are given by (58).

Proof: This is a special case of observation 3.1.1. □

Remark 3.3.1: In the ensuing analysis, we have assumed that the SVD of $\hat{\mathbf{B}}$ provides a sensible spectral basis for $\mathbf{Y}$, in the sense that $\mathbf{B}_r$ and $\hat{\mathbf{B}}_r$ are close for $r = 1, \ldots, r_c$, where $r_c \leq m$. For example, consider the case where r_c is chosen such that $\|\mathbf{B}_r - \hat{\mathbf{B}}_r\|_F$ is bounded for $r = 1, \ldots, r_c$, where $\|\cdot\|_F$ denotes the Frobenius norm. We have also assumed that closed-loop stability of (14) is ensured for chosen values of r.

In the light of observation 3.3.1, we offer one interpretation for the effect of model mismatch on steady-state performance. First, note that as the estimated model tends to the ideal model (in some sense), then $\hat{\mathbf{W}} \to \mathbf{W}$, $\hat{\mathbf{V}} \to \mathbf{V}$ and $\mathbf{F} \to \mathbf{0}$, in which case the analysis from Section 3.2 is directly applicable. Note that where it is convenient, we may refer to $\mathbf{F}$ as the leakage term. In the more general case where $\Delta \neq \mathbf{0}$ (refer to (63)), the leakage term is not necessarily of negligible effect. In fact, we verify by means of an upper bound for output variation, that as r increases, the leakage term becomes detrimental to steady-state performance.

The relationship between $\mathbf{F}$ and $\mathbf{H}$ is given by (68). From (62) we see that $\mathbf{H}$ is a function of $\mathbf{M}$, $\mathbf{S}$ and $\mathbf{N}$. Furthermore, $\mathbf{M}$ and $\mathbf{N}$ are unitary matrices that rotate $\hat{\mathbf{W}}$ into $\mathbf{W}$ and $\hat{\mathbf{V}}$ into $\mathbf{V}$, respectively. Therefore, the leakage term is intimately connected with model mismatch. This may be more clearly seen as follows. Let the first r columns of $\hat{\mathbf{W}}$ be denoted as $\hat{\mathbf{W}}_{uc_r}$, which we refer to as the uncontrolled basis functions. The remaining $n-r$ columns of $\hat{\mathbf{W}}$ are denoted as $\hat{\mathbf{W}}_{uc_r}$, which we refer to as the uncontrolled basis functions. Similarly, let $\hat{\mathbf{V}}_{c_r}$ denote the first r columns of $\hat{\mathbf{V}}$. We define $\mathbf{M}_{c_r}$, $\mathbf{M}_{uc_r}$ and $\mathbf{N}_{c_r}$ in the same manner. Three expressions for $\mathbf{H}_{11}$ and $\mathbf{H}_{21}$ are

$$\mathbf{H}_{11} = \hat{\mathbf{S}}_{11} - \hat{\mathbf{W}}_{c_r}^T \Delta \hat{\mathbf{V}}_{c_r} \qquad \mathbf{H}_{21} = -\hat{\mathbf{W}}_{uc_r}^T \Delta \hat{\mathbf{V}}_{c_r} \tag{69}$$

$$\mathbf{H}_{11} = \hat{\mathbf{W}}_{c_r}^T \mathbf{B} \hat{\mathbf{V}}_{c_r} \qquad \mathbf{H}_{21} = \hat{\mathbf{W}}_{uc_r}^T \mathbf{B} \hat{\mathbf{V}}_{c_r} \tag{70}$$

$$\mathbf{H}_{11} = \mathbf{M}_{c_r}^T \mathbf{S} \mathbf{N}_{c_r} \qquad \mathbf{H}_{21} = \mathbf{M}_{uc_r}^T \mathbf{S} \mathbf{N}_{c_r} \tag{71}$$

In the ideal case where $\hat{\mathbf{W}} = \mathbf{W}$ and $\hat{\mathbf{V}} = \mathbf{V}$, then $\mathbf{H}_{11} = \mathbf{S}_{11}$ and $\mathbf{H}_{21} = \mathbf{0}$. Therefore, we might expect that for Δ small, $\mathbf{H}_{11}$ and $\mathbf{H}_{21}$ behave in a similar manner to the ideal case, which implies that $\mathbf{F}$ would have negligible impact on $\mathbf{y}_{ss}$. Furthermore, when r is small, we might also expect that $\mathbf{F}$ has negligible effect on $\mathbf{y}_{ss}$ since this corresponds to the 'significant' singular-values. We illustrate these ideas with an example.

Example 2: Consider again the model of a paper machine with 101 actuators and 501 measurement points across the profile, with nominal bump response shape given as in Fig. 2*a*. We are concerned with three cases: (1) $\Delta = 0$, i.e. no model mismatch, (2) $\|\Delta\|_2 = 0.1$, where Δ is a random perturbation matrix, and (3) Δ is given by the difference between the nominal model $\mathbf{B}$ and an estimated model $\hat{\mathbf{B}}$ where the bump response shape has been deliberately stretched as seen in Fig. 3*a*, in this case the matrix norm is measured as $\|\Delta\|_2 \approx 2.2$.

In the first case, where there is no model mismatch, we see from Fig. 3*b* that the output variation is monotonically nonincreasing (see Section 3.2). In the second case, we see that for $r \lesssim 45$ the output variation closely matches the nominal case and increases rapidly for $r \gtrsim 80$. In the third case, we see that output variation closely matches the nominal case for $r \lesssim 15$ and increases sharply for $r \gtrsim 25$. In both cases of model mismatch, simulations have suggested that closed-loop stability is particularly hard to achieve after the point where the variation increases sharply.

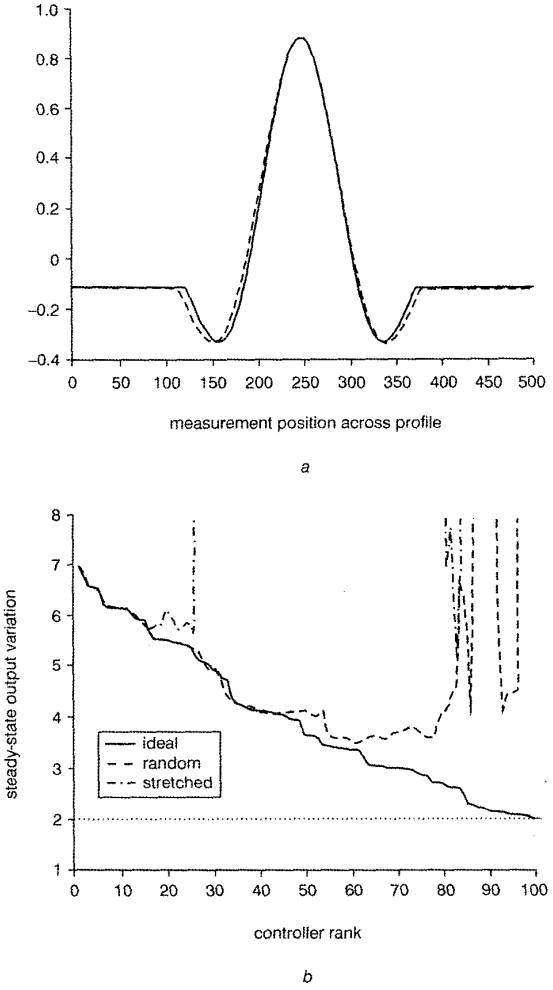

Fig. 3 *Steady-state variation with model mismatch*
closed loop stability is assumed, although simulations suggest that it is particularly hard to achieve after the variation increases sharply
a bump response shape from actuator no. 50 for nominal and estimated models. Shapes are constructed using a truncated sync function
—— nominal shape
– – – estimates shape
b steady-state output variation $\|\mathbf{y}_{ss}\|_2$ as a function of r
—— ideal case
– – – model mismatch with random perturbation matrix
– . – model mismatch with stretched actuator response
..... lower bound for output variation

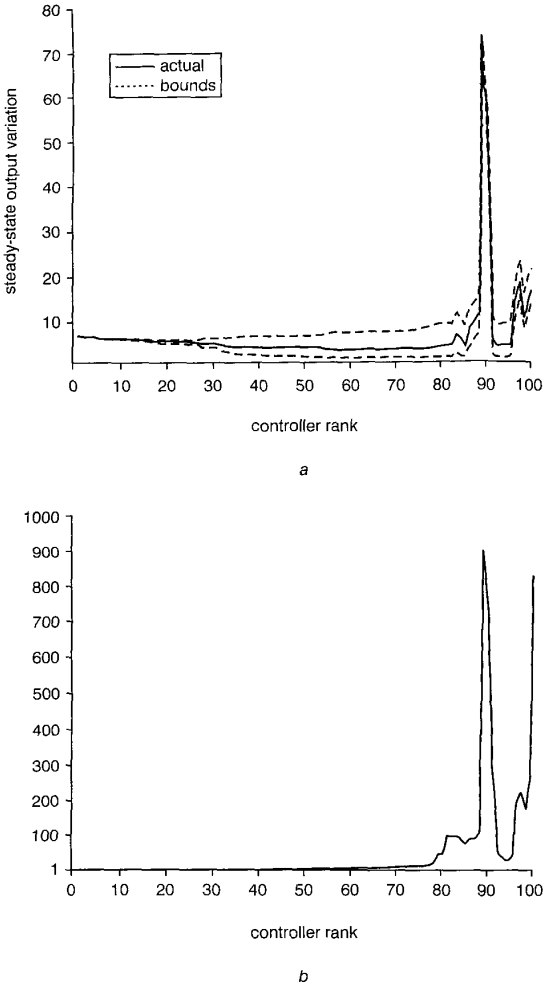

Fig. 4 *Bounds on steady-state output variation*
a upper and lower bounds for output variation
b norm of leakage term **F**

Using $\hat{\mathbf{W}}_{c_r}$ and $\hat{\mathbf{W}}_{uc_r}$ as defined above, we may express (66) as

$$\mathbf{y}_{ss} = \hat{\mathbf{W}}_{uc_r}[\mathbf{F}\hat{\mathbf{W}}_{c_r}^T\mathbf{d}_{ss} + \hat{\mathbf{W}}_{uc_r}^T\mathbf{d}_{ss}] \tag{72}$$

Observe that the first r modes of $\mathbf{y}_{ss}$, i.e. the controlled modes, are zero since $\hat{\mathbf{W}}_{c_r}^T\hat{\mathbf{W}}_{uc_r} = \mathbf{0}$. The remaining $n - r$ modes of $\mathbf{y}_{ss}$, i.e. uncontrolled modes, are a linear combination of the uncontrolled modes of $\mathbf{d}_{ss}$ and the controlled modes of $\mathbf{d}_{ss}$ mapped through **F**. We can use (72) to develop a bound for output variation. Note that

$$\|\mathbf{y}_{ss}\|_2 = \|\hat{\mathbf{W}}^T\mathbf{y}_{ss}\|_2 \tag{73}$$

$$= \|\hat{\mathbf{W}}_{uc_r}^T\mathbf{y}_{ss}\|_2 \tag{74}$$

since $\hat{\mathbf{W}}$ is unitary. Therefore, an upper bound for $\|\mathbf{y}_{ss}\|_2$ may be given by

$$\|\mathbf{y}_{ss}\|_2 \leq \|\mathbf{F}\hat{\mathbf{W}}_{c_r}^T\mathbf{d}_{ss}\|_2 + \|\hat{\mathbf{W}}_{uc_r}^T\mathbf{d}_{ss}\|_2 \tag{75}$$

Moreover, we can obtain a lower bound from the triangle inequality

$$\|\mathbf{y}_{ss}\|_2 \geq \left|\|\mathbf{F}\hat{\mathbf{W}}_{c_r}^T\mathbf{d}_{ss}\|_2 - \|\hat{\mathbf{W}}_{uc_r}^T\mathbf{d}_{ss}\|_2\right| \tag{76}$$

Let LB_{nom} denote the lower bound for output variation (see observation 3.1.2). Furthermore, let the right-hand side of (75) be denoted as UB_F and similarly the right-hand side of (76) as LB_F, then we have the following bound for $\|\mathbf{y}_{ss}\|_2$.

$$\min\{LB_{nom},\ LB_F\} \leq \|\mathbf{y}_{ss}\|_2 \leq UB_F \tag{77}$$

This bound is illustrated in Fig . 4*a*. In Fig. 4*b* we show the plot of $\|\mathbf{F}\|_2$. Note that the peak that is observed in Fig. 4*a* corresponds to the peak shown in Fig. 4*b*, hence illustrating the dependence of $\|\mathbf{y}_{ss}\|_2$ on **F**.

4 Conclusions

We have considered the steady-state behaviour of cross-directional control systems in a closed-loop. The linear unconstrained case provides a benchmark for performance analysis, even though this case is usually not attainable due to actuator constraints, the necessity for robustness, numerical considerations etc. It is usual to project the profile onto a reduced space which we have termed the controlled subspace. With integral action, the effects of both such a projection and model mismatch can be interpreted as leakage from the controlled disturbance modes to the uncontrolled output modes.

With no model mismatch it is well known that increasing the number of controlled modes should improve the steady-state performance. This result is readily extendible to the constrained case. But model mismatch tends to degrade performance; even under an assumption of stability this degradation may become overriding as the number of modes increases. We have put new bounds on the performance under such circumstances. While the extension of such results to the constrained case does not appear to be straightforward, the conclusion is clear: improved knowledge of the plant should lead to improved steady-state performance.

5 References

1 LEVY, S., and CARLEY, J.F.: 'Plastics extrusion technology handbook' (Industrial Press, New York, 1989, 2nd edn.)
2 SMOOK, G.A.: 'Handbook for Pulp and Paper Technologists' (Tappi, Atlanta, 1982)
3 DUNCAN, S.R., and BRYANT, G.F.: 'The spatial bandwidth of cross-directional control systems for web processes', *Automatica*, 1997, **33**, (2), pp. 139–153
4 HEATH, W.P.: 'Orthogonal functions for cross-directional control of web-forming processes', *Automatica*, 1996, **32**, (2), pp. 183–198
5 KRISTINSSON, K., and DUMONT, G.A.: 'Paper machine crossdirectional basis weight control using gram polynomials'. Proceedings of the 2nd IEEE Conference on Control applications, Vancouver, British Columbia, 1993, pp. 235–240
6 HALOUSKOVA, A., KARNY, M., and NAGY, I.: 'Adaptive cross-direction control of paper basis weight', *Automatica*, 1993, **29**, (2), pp. 425–429
7 STEWART, G.E.: 'Two dimensional loop shaping controller design or paper machine cross-directional processes'. 2000, PhD thesis, University of British Columbia
8 FEATHERSTONE, A.P., VANANTWERP, J.G., and BRAATZ, R.D.: 'Identification and control of sheet and film processes' (Springer-Verlag, London, 2000)
9 DUNCAN, S.R., and CORSCADDEN, K.W.: 'Mini-max control of cross-directional variations on a paper machine', *IEE Proc., Control Theory Appl.*, 1998, **145**, (2), pp. 189–195
10 DUNCAN, S.R.: 'The cross-directional control of web-forming processes'. 1989, PhD thesis, University of London
11 LJUNG, L.: 'System identification: theory for the user', 2nd edn. (Prentice-Hall, Upper Saddle River, NJ, 1999.)
12 STEWART, G.E., GORINEVSKY, D.M., DUMONT, G.A., GHEORGHE, C., and BACKSTROM, J.U.: 'The role of model uncertainty in cross directional control systems', *Proceedings of Control Systems 2000, Victoria, BC*, 2000, pp. 337–345
13 GOLUB, G.H., and VAN LOAN, C.F.: 'Matrix computations' (The Johns Hopkins University Press, 1996)
14 CAMPBELL, J.C., and RAWLINGS, J.B.: 'Predictive control of sheet and film-forming processes', *AIChE J*, 1998, **44**, (8)
15 CLARKE, D.W., MOHTADI, C., and TUFFS, P.S.: 'Generalized predictive control, parts 1 and 2', *Automatica*, 1987, **23**, (2), pp. 137–148
16 MUSKE, K.R., and RAWLINGS, J.B.: 'Model predictive control with linear models', *AIChE J*, 1993, **39**, (2), pp. 262–287